

Automated detection of lung tumors in PET/CT images using active contour filter

Atsushi Teramoto^{*a}, Hayato Adachi^a, Masakazu Tsujimoto^a, Hiroshi Fujita^b, Katsuaki Takahashi^c, Osamu Yamamuro^c, Tsuneo Tamaki^c, Masami Nishio^d, Toshiki Kobayashi^d

^aGraduate School of Health Sciences, Fujita Health University,
1-98 Dengakugakubo, Kutsukake-cho, Toyoake-city, Aichi 470-1192, Japan;

^bDepartment of Intelligent Image Information, Division of Regeneration and Advanced Medical Sciences, Graduate School of Medicine, Gifu University,
1-1 Yanagido, Gifu 501-1194, Japan;

^cEast Nagoya Imaging Diagnosis Center,
3-4-26 Jiyugaoka, Chikusa-ku, Nagoya 464-0044, Japan;

^dNagoya Radiological Diagnosis Center
1-162 Hokke, Nakagawa-ku, Nagoya 454-0933, Japan.

ABSTRACT

In a previous study, we developed a hybrid tumor detection method that used both computed tomography (CT) and positron emission tomography (PET) images. However, similar to existing computer-aided detection (CAD) schemes, it was difficult to detect low-contrast lesions that touch to the normal organs such as the chest wall or blood vessels in the lung. In the current study, we proposed a novel lung tumor detection method that uses active contour filters to detect the nodules deemed "difficult" in previous CAD schemes. The proposed scheme detects lung tumors using both CT and PET images. As for the detection in CT images, the massive region was first enhanced using an active contour filter (ACF), which is a type of contrast enhancement filter that has a deformable kernel shape. The kernel shape involves closed curves that are connected by several nodes that move iteratively in order to enclose the massive region. The final output of ACF is the difference between the maximum pixel value on the deformable kernel, and pixel value on the center of the filter kernel. Subsequently, the PET images were binarized to detect the regions of increased uptake. The results were integrated, followed by the false positive reduction using 21 characteristic features and three support vector machines. In the experiment, we evaluated the proposed method using 100 PET/CT images. More than half of nodules missed using previous methods were accurately detected. The results indicate that our method may be useful for the detection of lung tumors using PET/CT images.

Keywords: Lung tumor, PET/CT, Computer-aided detection (CAD), Detection, Active contour

1. INTRODUCTION

Lung cancer is the leading cause of death among men worldwide [1]. Consequently, early detection is essential to decrease the number of cancer-related deaths. X-ray computed tomography (CT) was recently adopted as a mass-screening tool for lung cancer diagnosis [2], enabling rapid improvement in the ability to detect tumors early. According to the results from the National Lung Screening Trial [3], screening using low-dose CT decreases the incidence of lung cancer-related deaths among smokers by 20%. A greater number of CT examinations are expected to be adopted for lung screening in the future. Of late, positron emission tomography (PET)/CT is being used as a cancer-screening tool [4,5]. PET/CT is an imaging technique that provides both functional and anatomical information; therefore, it is useful for the early detection of lung cancer. However, radiologists must examine a large number of images. Computer-aided detection (CAD) provides a computerized output as a second opinion to support a radiologist's diagnosis and is expected to assist radiologists who are required to evaluate a large number of images to identify lesions and arrive at a diagnosis. In this study, we focused on the automated detection of lung tumors using PET/CT.

In a previous study, we developed an automated lung nodule detection scheme that entailed the use of both CT and PET [6]. The detection sensitivity was 83.0%, and the corresponding number of false-positive (FP) detections per case was 5.0. However, similar to the issues faced with existing CAD schemes, it was difficult to detect low-contrast lesions in contact with normal organs such as the chest wall or blood vessels in the lung. In this paper, we propose a novel lung tumor detection method that involves the use of active contour filters to detect nodules that could not be identified using previous CAD schemes.

2. METHODS

2.1 Image dataset

A total of 104 Japanese men and women who underwent whole-body PET/CT during cancer screening programs from 2009 to 2012 were included in this study. Scanning was performed using a SIEMENS unit (Truepoint Biograph 40) with standard settings that are routinely used in the clinic. The spatial resolution of the PET images was $4.0 \times 4.0 \times 2.0 \text{ mm}^3$, while that of the CT images was $0.97 \times 0.97 \times 2.0 \text{ mm}^3$. A total of 179 nodules were detected in 84 patients.

This study was approved by our institutional review board, and patient agreement was based on the assumption that all data were anonymized.

2.2 Methods outline

The proposed scheme, as shown in Figure 1, was designed to detect lung tumors using both CT and PET. First, nodules and masses were identified separately on the PET and CT images using the specific features of each image. Subsequently, the PET and CT images of candidate lesions were combined. FPs were eliminated using the hybrid FP reduction technique. Finally, candidate regions for the tumors were recorded. The detection and integration methods are described below.

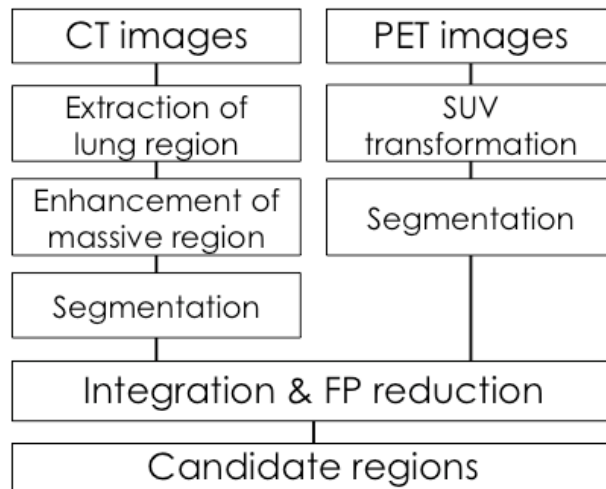


Fig. 1 Flow chart for the proposed method.

2.3 Detection using CT

First, the lung region on the CT images was automatically segmented by thresholding and three-dimensional morphological operations. Then, the massive region was enhanced using selective enhancement filters. In our previous study, we used cylindrical filters for enhancement [7]. However, it was difficult to detect low-contrast lesions in contact with normal organs such as the chest wall or blood vessels in the lung. Therefore, in this study, we developed an active contour filter (ACF), which is a type of contrast enhancement filter with a deformable kernel shape. The kernel shape includes closed curves that are connected by several nodes that move iteratively in order to enclose a massive region, such as nodules or masses (Fig. 2). The final output of ACF is the difference between the maximum pixel value on the

deformable kernel and the pixel value on the center of the filter kernel. Figure 3 shows the behavior of ACF when used with a digital phantom. Then, initial candidates were obtained by thresholding and labeling processing.

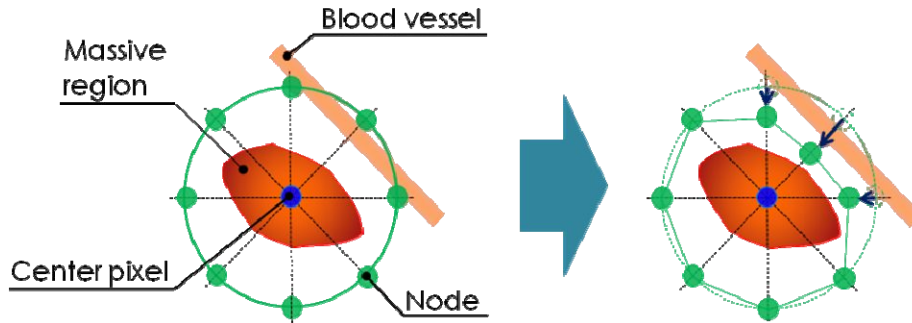


Fig. 2 Structure and deformation of an active contour filter

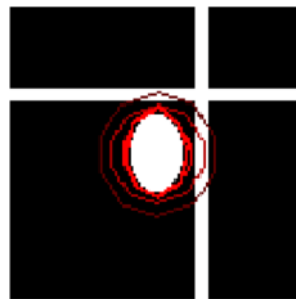


Fig. 3 Deformation of the contour in an active contour filter. This image simulates an oval nodule surrounded by blood vessels (white objects). The red lines show the active contours, while the bright curve around the oval nodule is the final shape of the filter kernel.

2.4 Detection using PET

The PET images were subsequently binarized using a predetermined threshold to detect regions of increased uptake. The PET images show the tissue radioactivity concentration. However, this varies with the injected dose and patient's weight. Therefore, the standardized uptake value (SUV) is calculated for each image as the ratio of the measured activity to the injected dose/patient body weight [8].

$$SUV = \frac{\text{Measured activity}[Bq / mL]}{\text{Injected dose}[Bq] / \text{body weight}[g]} \quad (2)$$

Then, the images were enhanced using three-dimensional iris filters, followed by the identification of candidate lesions using thresholding. The heart, liver, and kidneys showed physiological uptake adjacent to the lungs. Candidate regions other than the lungs were eliminated using the lung regions recorded on the CT images.

2.5 Integration and FP reduction

Initial candidate regions detected on CT and PET were represented as binary images. The two images were then combined using logic OR. Following pixel-by-pixel confirmation of regions on both images, the region detected by at least one modality was treated as an initial candidate region. Although an improvement in sensitivity was expected after combination of the two modalities, an increase in FPs was a challenge at the same time. There were approximately 100

FPs per case for the initial combined candidates. Therefore, FP reduction was performed using multiple characteristic features and multi-step classifiers using a rule-based classifier and three support vector machines (SVMs; Fig. 4) [9].

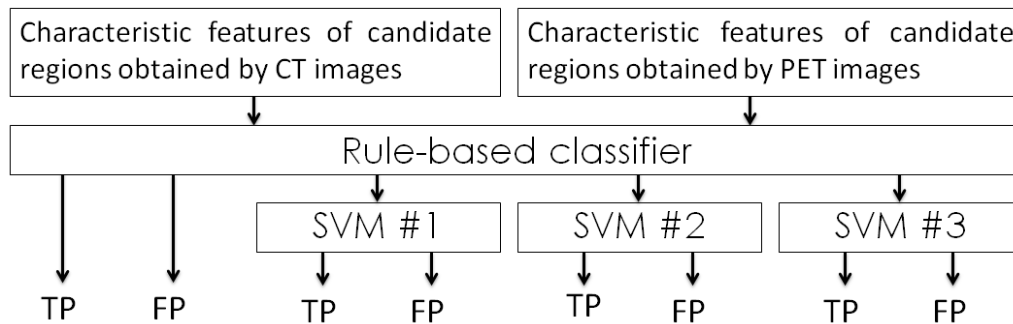


Fig.4 Flow chart of FP reduction method

3. EXPERIMENTS

To evaluate the effectiveness of the proposed method, we assessed the PET/CT images obtained for the 104 patients. The data pertaining to candidate regions were randomly divided into five datasets and evaluated using the cross-validation method. With regard to the detection parameters, the maximum filter radius of ACF was set at 25 mm, while the number of nodes was set at eight. For detection on PET, the threshold was set at 2.0. We introduced the LibSVM for FP reduction [10]; C-SVC with the kernel of the radial basis function was introduced. Image data were processed using in-house CAD software (Fig. 5) using a 3.06-GHz XEON processor (12 cores) with a 32.0-GB memory.

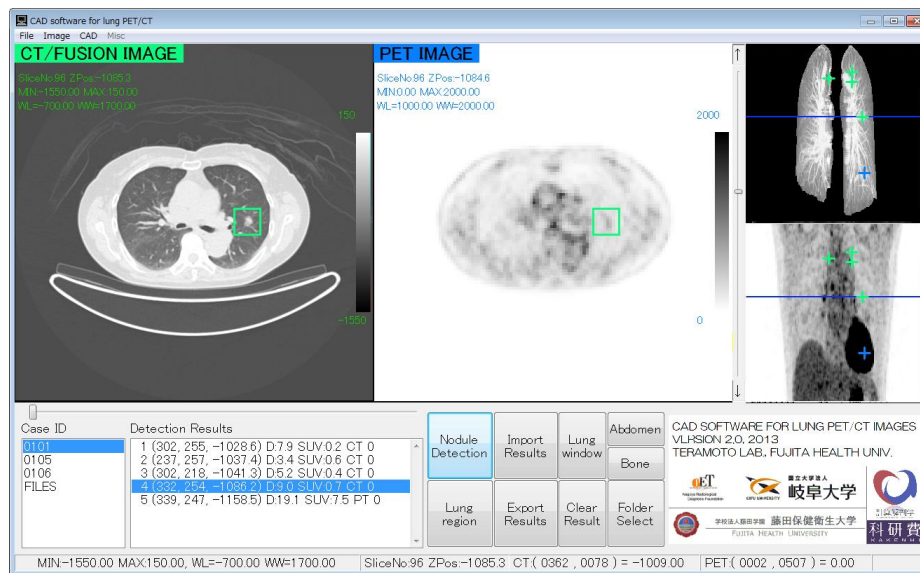


Fig.5 CAD software

Figure 6 shows the newly detected tumors using our proposed method, which also detected nodules adjacent to normal organs, as opposed to our previous method.

Figure 7 shows the FROC curves of our proposed method. The true-positive fraction (TPF) for the detection of nodules using CT only was 0.810, while the FP/case was 6.1. The combination of CT and PET improved TPF to 0.893, with an FP/case of 6.1. Therefore, the sensitivity of our proposed hybrid method was superior to that of individual detection.

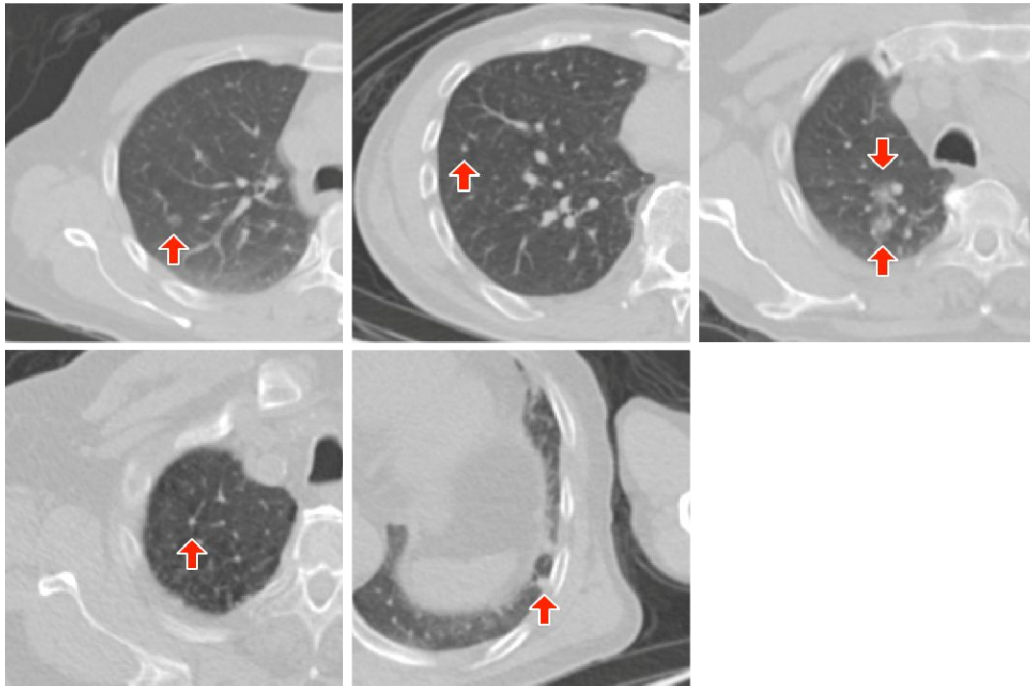


Fig. 6 Newly detected nodules using our proposed method. The arrows indicate the nodules.

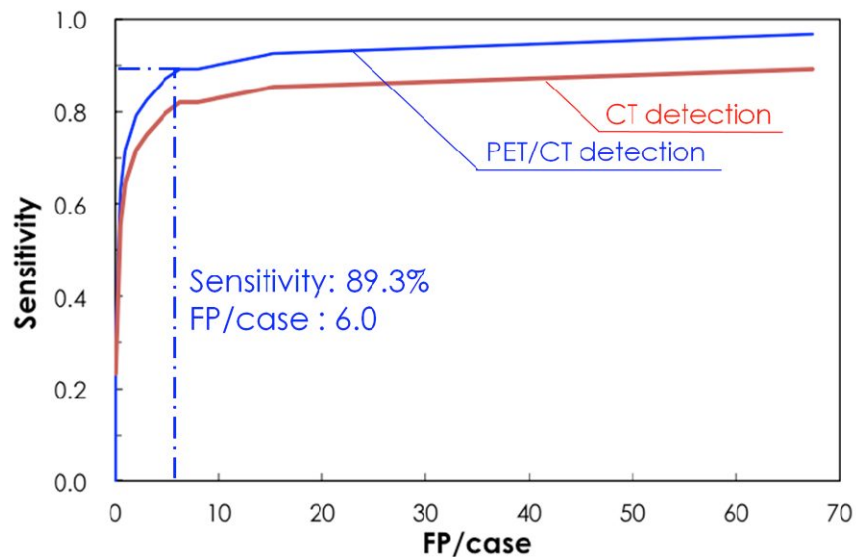


Fig.7 FROC curves for CT (red) and PET/CT (blue) detection algorithm.

4. CONCLUSIONS

In this study, we developed a novel lung tumor detection method using PET/CT and the use of ACFs to detect nodules that were difficult to identify using previous CAD schemes. Many nodules overlooked using previous methods were accurately detected using our proposed method. In summary, our hybrid method involving PET/CT may be useful for early and accurate lung tumor detection.

ACKNOWLEDGMENT

This research was granted in part by a Grant-in-Aid for Scientific Research on Innovative Areas, MEXT, Japan; in part by Tateishi Science and Technology Foundation, Japan.

REFERENCES

- [1] Ferlay, J, Shin, HR, Bray, F, Forman, D, Mathers, C and Parkin, DM, "GLOBOCAN 2008 v2.0, cancer incidence and mortality worldwide," IARC CancerBase 10, <http://globocan.iarc.fr>
- [2] Sone, S, Takashima, S, Li, F, Yang, Z, Honda, T, Maruyama, Y, et al., "Mass screening for lung cancer with mobile spiral computed tomography scanner," *Lancet* 351, 1242-1245(1998).
- [3] National Lung Screening Trial. Information is available at <http://www.cancer.gov/clinicaltrials/noteworthy-trials/nlst>
- [4] Lee, JW, Kang, KW, Paeng, JC, Lee, SM, Jang, SJ, et al., "Cancer screening using 18F-FDG PET/CT in Korean asymptomatic volunteers: A preliminary report," *Ann Nucl Med* 23(7), 685-691 (2009).
- [5] Ide, M and Suzuki, Y, "Is whole-body FDG-PET valuable for health screening?," *Eur J Nucl Med Mol Imaging* 32(3), 339-341 (2005).
- [6] Teramoto, A, Fujita, H, Takahashi, K, Yamamuro, O, et al., "Hybrid method for the detection of pulmonary nodules using positron emission tomography / computed tomography: A preliminary study," *IJCARS* 9(1), 59-69 (2014).
- [7] Teramoto, A and Fujita, H, "Fast lung nodule detection in chest CT images using cylindrical nodule-enhancement filter," *IJCARS* 8(2), 182-205 (2013).
- [8] Keyes, JW, "SUV: Standard uptake or silly useless value?," *J Nucl Med* 36(10), 1836-1839 (1995).
- [9] Cristianini, N, Shawe-Taylor J, "An introduction to support vector machines and other kernel-based learning methods," Cambridge University Press, Cambridge (2000).
- [10] Chang, C.C., Lin, C.J., "LIBSVM: a library for support vector machines," Software available at <http://www.csie.ntu.edu.tw/~cjlin/libsvm/>